CALCULATION OF TURBULENT REACTING FLOWS IN A CYLINDRICAL COMBUSTOR WITH SWIRLING INFLOWS

Xue-Song Bai and Laszlo Fuchs,
Dept. of Heat and Power Engineering/Fluid Mechanics
Lund Institute of Technology, S-221 00 Lund, Sweden

Abstract

This paper presents the calculation of turbulent reacting flows in a cylindrical combustor, where the flame is stabilized by inlet swirling. Such type of flows exhibits considerable difficulties due to highly rotational and non-isotropic characters of the turbulent motion. In this paper a linear $k-\epsilon$ model, a non-linear $k-\epsilon$ model and a Large Eddy Simulation (LES) model are employed. The mean tangential velocity and the root-mean-square axial- and tangential- velocity fluctuations are predicted qualitatively well by the two $k-\epsilon$ models, as compared to the measured data. However, the mean axial- (and radial-) velocity components and thus the recirculation zones are poorly calculated by the $k-\epsilon$ models. Both $k-\epsilon$ models produce a steady axisymmetric flow field. Some preliminary LES calculations are also presented.

1 Introduction

Swirling stabilized flames are commonly seen in practical combustion devices. Such flames are found to be quite sensitive to the operation and geometric conditions, such as inlet swirl number, pressure and the ratio of fuel/air inlet velocities [1]. Experimental and theoretical investigations of swirling flows have been reported in the literature, for both chemically reacting and non-reacting flows [1-3].

Numerical simulation of these types of flow is challenging due to the fact that the rotational flow structure exhibits a highly anisotropic character and therefore the conventional methods such as a linear $k-\epsilon$ model is unable to properly reproduce the flow situation. In order to account for the anisotropic nature of most turbulent flows, modifications of the the linear $k-\epsilon$ model has been suggested [4-6]. The Reynolds stresses are modeled by a more general relation of the mean strain rate tensor and the mean rotation tensor. Calculations of turbulent flows in a rectangular duct show that the non-linear $k-\epsilon$ model is able to capture the secondary flows, while the linear model fails [6]. In this work, the linear $k-\epsilon$ model and a non-linear $k-\epsilon$ model are used to compute the mean field in the case of reacting flows. A "static" LES model is used to further study the details of the fluctuations in swirling (cold) flows.

Current understanding of the combustion processes in practical combustors (such as gas turbine combustors) has shown that the interaction between chemical kinetics and fluid flow (often turbulent) plays an important role in the overall performance of the combustors. Turbulence not only improves the mixing of the fuel and oxidant, but also may quench or accelerate the reactions. Several models have been proposed in the literature for handling the interactions between turbulence and chemical reactions, e.g., the Eddy Dissipation Concept (EDC) model [7]; Probability Density Function (PDF) method [8]; Flamelet method [9,10]. Sensitivity study of different models has shown that although the minor species are fairly sensitive to different models, the major species and velocity field are less sensitive to the choice of the sub-models. Since the aim of this paper is to examine how well the flow field is modeled by different approaches, we chose the EDC model [7] for simplicity.

The model equations for the reacting flows are the Favre averaged/filtered Navier-Stokes equations and energy and species transport equations. The set of partial differential equations are solved numerically by using high order finite difference scheme. The numerical results, when compared to the experimental data show the shortcomings of the linear and the non-linear $k-\epsilon$ models for highly swirling flows. It is believed that LES will be able to handle such flows with a considerably better accuracy. However, the current amount of data is not adequate as yet to compare turbulence details using the current LES.

2 FORMULATIONS

The governing equations for turbulent reaction flows are the Navier-Stokes equations together with the continuity equation, and transport equations for energy and chemical species. Let $\overline{\phi}$ denote the time averaging (for $k-\epsilon$ models) or space filtering (for LES) of variable ϕ. In cartesian coordinates the averaged (filtered) governing equations can be written as

Continuity

$$\frac{\partial \overline{\rho}}{\partial t} + \frac{\partial \overline{\rho u_j}}{\partial x_j} = 0, \tag{1}$$

Momentum

$$\frac{\partial \overline{\rho u_i}}{\partial t} + \frac{\partial \overline{\rho u_j u_i}}{\partial x_j} = -\frac{\partial \overline{p}}{\partial x_i} + \tag{2}$$

$$\frac{\partial}{\partial x_j}[\overline{\mu(\frac{\partial u_i}{\partial x_j} + \frac{\partial u_j}{\partial x_i} - 2/3\delta_{ij}\frac{\partial u_k}{\partial x_k})}],$$

Energy

$$\frac{\partial \overline{\rho h}}{\partial t} + \frac{\partial \overline{\rho u_j h}}{\partial x_j} = \frac{\partial}{\partial x_j}(\overline{\frac{\mu}{Pr}\frac{\partial h}{\partial x_j}}) + \frac{\partial \overline{p}}{\partial t}, \tag{3}$$

Species

$$\frac{\partial \overline{\rho Y_i}}{\partial t} + \frac{\partial \overline{\rho u_j Y_i}}{\partial x_j} = \frac{\partial}{\partial x_j}(\overline{\rho D\frac{\partial Y_i}{\partial x_j}}) + \overline{w_i}, \tag{4}$$

where ρ is density and t is time; u_j are the velocity components in cartesian coordinates x_j directions, respectively. μ is the laminar viscosity; p is the pressure; Pr is the Prandtl number.

The enthalpy h is defined by

$$h = Y_i(H_i^0 + \int_{T_0}^{T} C_{P_i} d\tau), \tag{5}$$

where H_i^0 is the enthalpy of formation at reference temperature T_0. T is the gas temperature; C_{Pi} is the specific heat capacity for species i. Y_i is the mass fraction of species i; D is the mass diffusivity; w_i is the reaction rate of species i.

2.1 LINEAR AND NON-LINEAR $k-\epsilon$ MODELS

By using Favre decomposition, one can write

$$u_i = \widetilde{u_i} + u_i'', \quad \phi = \widetilde{\phi} + \phi'', \tag{6}$$

where

$$\widetilde{u_i} = \frac{\overline{\rho u_i}}{\overline{\rho}}, \quad \widetilde{\phi} = \frac{\overline{\rho\phi}}{\overline{\rho}}. \tag{7}$$

Here ϕ represents h and Y_i.

For statistically stationary flows, the time averaged unknown terms $\overline{\rho u_j u_i}$ and $\overline{\rho u_j \phi}$ can be written as

$$\overline{\rho u_j u_i} = \overline{\rho}\widetilde{u_j}\widetilde{u_i} + \overline{\rho u_i'' u_j''}$$

$$\overline{\rho u_j \phi} = \overline{\rho}\widetilde{u_j}\widetilde{\phi} + \overline{\rho\phi'' u_j''}$$

In the linear $k-\epsilon$ model, the unknown Reynolds stresses are modeled based on the Boussinesq hypothesis

$$-\overline{\rho u_i'' u_j''} = \mu_t(\frac{\partial \widetilde{u_i}}{\partial x_j} + \frac{\partial \widetilde{u_j}}{\partial x_i}) - \frac{2}{3}\delta_{ij}(\overline{\rho}k + \mu_t\frac{\partial \widetilde{u_l}}{\partial x_l}) \tag{8}$$

where $k = \widetilde{u_i'' u_i''}/2$ is the turbulent kinetic energy. μ_t is the eddy viscosity. Similarly, a gradient diffusion model based on the eddy viscosity may be used for the turbulent scalar fluxes:

$$-\overline{\rho u_i'' Y_j''} = \frac{\mu_t}{Sc_t}\frac{\partial \widetilde{Y_j}}{\partial x_i}, \quad -\overline{\rho u_i'' h''} = \frac{\mu_t}{Pr_t}\frac{\partial \widetilde{h}}{\partial x_i} \tag{9}$$

where Sc_t and Pr_t are the turbulent Schmidt and Prandtl numbers, respectively.

For the $k-\epsilon$ models the eddy viscosity is computed by

$$\mu_t = C_\mu \overline{\rho}\frac{k^2}{\epsilon}. \tag{10}$$

C_μ is an experimentally determined constant ($C_\mu \sim 0.09$). The turbulent kinetic energy k and its dissipation rate ϵ are computed through transport equations.

In the non-linear $k-\epsilon$ model the Reynolds stresses are modeled by (cf. [6]):

$$-\overline{\rho u_i'' u_j''} = \mu_t(\frac{\partial \widetilde{u_i}}{\partial x_j} + \frac{\partial \widetilde{u_j}}{\partial x_i}) - \frac{2}{3}\delta_{ij}(\overline{\rho}k + \mu_t\frac{\partial \widetilde{u_l}}{\partial x_l}) \tag{11}$$

$$+4C_D C_\mu^2\frac{k^3}{\epsilon^2}(\widetilde{S}_{ik}\widetilde{S}_{kj} - \frac{1}{3}\widetilde{S}_{mn}\widetilde{S}_{mn}\delta_{ij})$$

$$+4C_D C_\mu^2\frac{k^3}{\epsilon^2}(\widetilde{S}_{ik}\widetilde{\omega}_{kj} + \widetilde{S}_{jk}\widetilde{\omega}_{ki}),$$

where $S_{ij} = 1/2(\partial u_i/\partial x_j + \partial u_j/\partial x_i)$ and $\omega_{ij} = 1/2(\partial u_i/\partial x_j - \partial u_j/\partial x_i)$ are the deformation- (symmetric) and rotation-tensors (skew-symmetric), respectively. The model constant C_D is taken to be 1.68.

2.2 LES MODEL

In LES models the space averaged non-linear terms can be written

$$\overline{\rho u_j u_i} = \overline{\rho}\widetilde{u_j}\widetilde{u_i} + \tau_{ij}$$

where τ_{ij} is the sub-grid stress (SGS). Smagorinsky SGS model is

$$\tau_{ij} - 1/3\delta_{ij}\tau_{ll} = -2\mu_\tau \widetilde{S}_{ij}$$

where

$$\mu_\tau = C\Delta^2\overline{\rho}|\widetilde{S}_{ij}|$$

Δ is the filter width. $C \sim 0.04$ is a model constant.

The Smagorinsky SGS model is often too dissipative and it is unable to model the energy transfer from

small scales to large scales (back-scattering). One may decrease the model constant C to minimize the dissipation and as it is done here, we use $C = 0$. The SGS effect is implicitly modeled by the numerical viscosities (which is of higher order than the Smagorinsky SGS model).

To properly model the back-scattering process, different models may be used, e.g. a dynamic SGS model [11-12]. One may also derive an explicit expression for the SGS [13]. This expression can be easily implemented for wall-free flows, but it will require further evaluation for wall bounded turbulence simulations.

2.3 Chemical reaction models

A simple one-step reaction scheme is used here (assuming that the fuel is methane):

$$CH_4 + 2(O_2 + 3.76N_2) \rightarrow CO_2 + 2H_2O + 7.52N_2$$

The Eddy Dissipation Concept (EDC) model is used to model the averaged reaction rate

$$\overline{w_f} = -A\bar{\rho}(\epsilon/k)min(\widetilde{Y_f}, \widetilde{Y_{O_2}}/4)$$

$$\overline{w_{O_2}} = 4\overline{w_f}$$

Here the subscript f denotes the fuel species and O_2 for the O_2 species. $A \approx 0.75$ is the value used for the model constant.

2.4 Numerical methods

The calculations using $k-\epsilon$ models are performed on a cylindrical coordinate system. Second order finite difference scheme is used: all terms with the exception of the convective terms are approximated by central differences. The convective terms in all the equations are approximated by second order upwind differences, in a "defect-correction" manner. Near wall boundaries central differences are used also for the convective fluxes. To enhance stability of the iterative procedure a quasi-time marching technique is employed. Details are given in [10].

The LES calculations are performed on cartesian grids. Third order finite difference scheme is used: all terms with the exception of the convective terms are approximated by fourth order finite differences. The convective terms in all the equations are approximated by third order upwind differences [11]. A backward Euler scheme is used for time integration. A Multi-Grid method is used to accelerate the convergence with each time step and a local grid refinement technique is used to obtain an optimal distribution of computational grids.

In both codes staggered grids are used.

3 Numerical simulations

The experimental setup of Owen et. al. [1] has been chosen in these calculations. The experimental rig consists of a 12.2 cm-diameter water-cooled, axisymmetric combustor in which a central fuel jet (supply CH_4) mixed with a heated (750 K) coaxial annular air stream. The test pressure was 3.9 atm. Flame stabilization was achieved by producing recirculation zones in the inital region of the combustor by high ratio of air/fuel inlet velocities (20:1) and by imparting a swirl component to the air flow.

A non-swirling case of the same combustor has been investigated previously by employing the linear $k-\epsilon$ model. The standard linear $k-\epsilon$ model produced qualitatively good results as compared with experimental data. Details of the calculation have been reported in paper [10]. Here we consider the swirling case. In this calculation, the computational grid was 82×42×3, i.e., axisymmetry is assumed. In LES calculations, a 3-D grid is used; the total number of grid cells is 1.9 million.

In the following calculation, the swirl number is 0.3 (the swirl number is defined as the ratio of the angular momentum flux to the axial momentum flux multiplied by an effective nozzle diameter [1]).

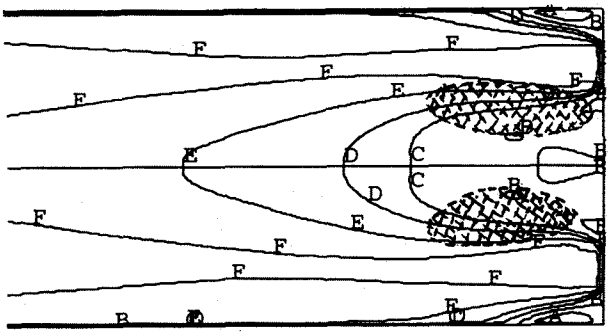

Figure 1: Iso-contours of mean axial velocity component. The shadowed regions represent the backflow region measured. The inlet turbulent intensity is $I = 10\%$ and the integral length scale 0.6 m. Line A, $\widetilde{u} = -2$; B, 0; C, 2; D, 4; E, 8; F, 14; unit m/s.

3.1 The $k-\epsilon$ calculations

Fig.1 shows the iso-contours of the Favre averaged mean axial velocity component field computed by the linear $k-\epsilon$ model. To compare with the measurement, the measured region where the axial velocity is negative (we refer to it here as the backflow region) is marked by shadows. Note that the computed back-

flow region (enclosed by iso-contour level B) is fairly different from that obtained from the measurements. We noticed that in the case without swirl, the backflow region is at the combustor axis and in the corner between the cylinder outer-wall and inlet plane [10]. With swirling inlet flow, the backflow region near the outer-wall disappeared, and the near axis recirculation region is pushed away from the axis by the centrifugal force. This feature is not predicted properly by the linear $k-\epsilon$ model, as shown in Fig.1: the outer-wall recirculation region is still fairly large and the near axis back flow is fairly weak and close to the axis.

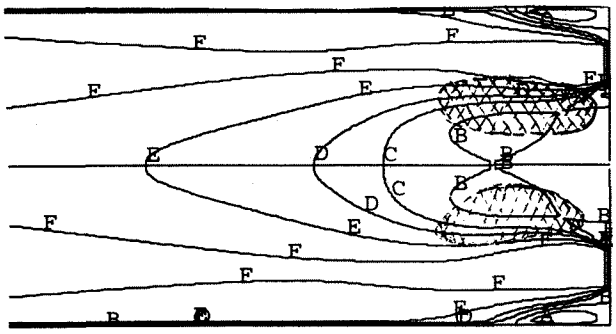

Figure 2: Iso-contours of mean tangential velocity component. The shadowed regions represent the backflow region measured. The inlet turbulent intensity is $I = 10\%$ and the integral length scale 0.6 m. Line A, $\widetilde{u} = -2$; B, 0; C, 2; D, 4; E, 8; F, 14; unit m/s.

Fig.2 shows the nonlinear $k-\epsilon$ results. As seen, the size and the location of the backflow recirculation region computed is fairly different from the measurement, even though a somewhat larger backflow region is found near the axis. The outer-wall recirculation zone is fairly strong too. In the above calculation, the inlet turbulent intensity is assumed to be $I = 10\%$ and the integral length scale is assumed to be 0.06 m (about the combustor radius). The influence of these inlet turbulent properties has been investigated, and further comparisons between the calculations and measurement are shown in Figs. 3-6.

Fig.3 shows the mean axial velocity distribution along the radial direction at three different axial positions: $x/D = 0.3$, 0.7 and 1.48. In the figure, the results using linear and non-linear $k-\epsilon$ models under two different inlet turbulence intensity levels ($I = 10\%$ and $I = 20\%$) are shown, together with the measured data. As seen, linear and nonlinear $k-\epsilon$ models give different results, which, however, are not very close to the experimental data (as also indicated in Figs. 1 and 2.)

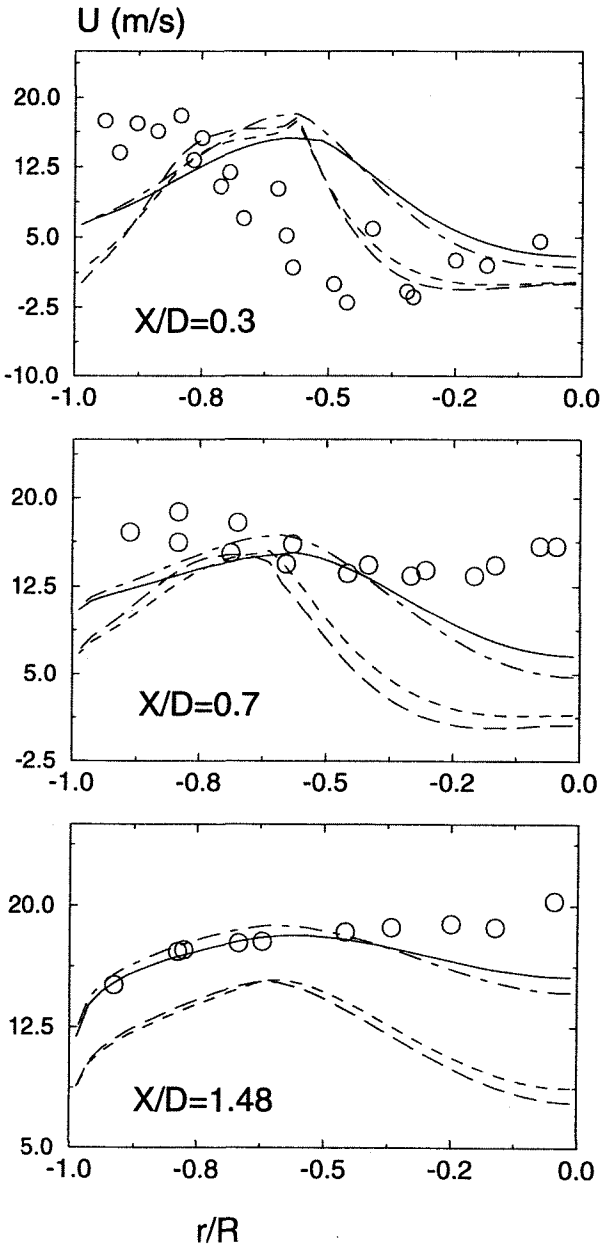

Figure 3: Mean axial velocity component along the radial direction at axial positions $x/D = 0.3, 0.7$ and 1.48. D is the diameter of the combustor. The circles represent the experimental data; the solid lines for the linear $k-\epsilon$ model at the inlet turbulent intensity $I = 20\%$; the dash-dot lines for the nonlinear $k-\epsilon$ model at the inlet turbulent intensity $I = 20\%$; the dashed lines for the linear $k-\epsilon$ model at the inlet turbulent intensity $I = 10\%$; and the long dashed lines for the nonlinear $k-\epsilon$ model at the inlet turbulent intensity $I = 10\%$.

Due to the erroneous backflow regions computed by

both models, the axial velocity near the combustor axis and the outer-wall ($r/R = 1$) are fairly different from the measurements, in particular at near inlet regions. The results show that the inlet turbulence level has a fairly large influence on the results.

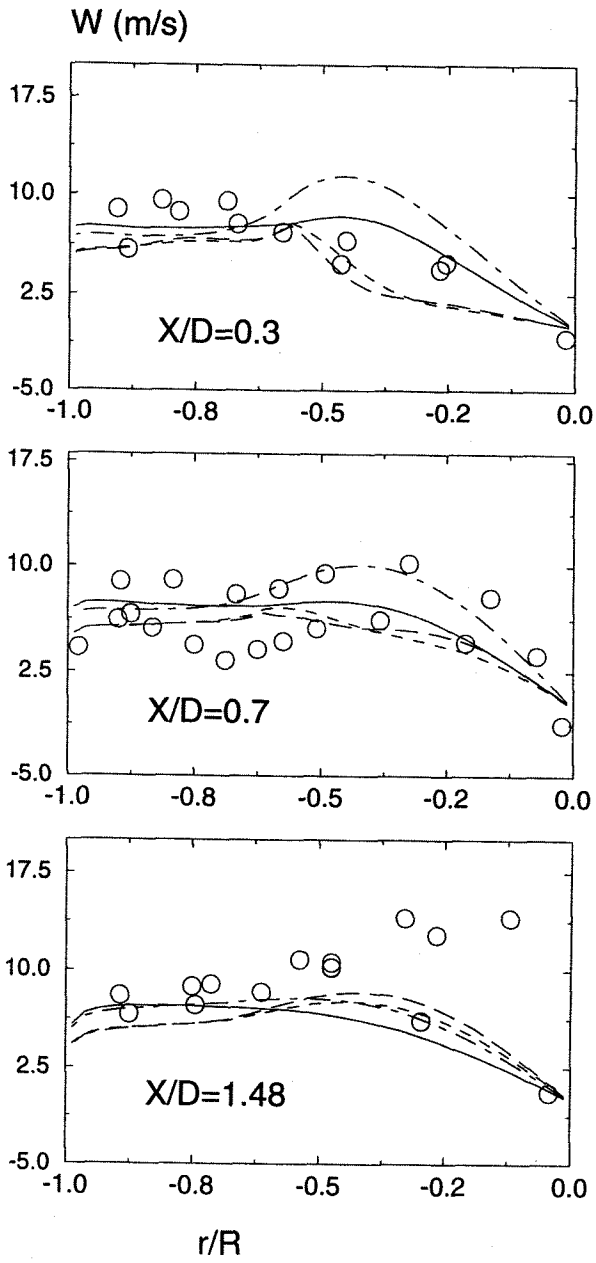

Figure 4: Mean tangential velocity component along the radial direction at axial positions $x/D = 0.3, 0.7$ and 1.48. The captions of the different lines and symbols are identical to those in Fig.3.

Fig.4 shows the tangential velocity component along the radial direction at the same three axial positions. As seen, both linear and non-linear $k-\epsilon$ models give results qualitatively close to the experimental data. Also the influence of inlet turbulence level on the tangential velocity is less important than on the axial component.

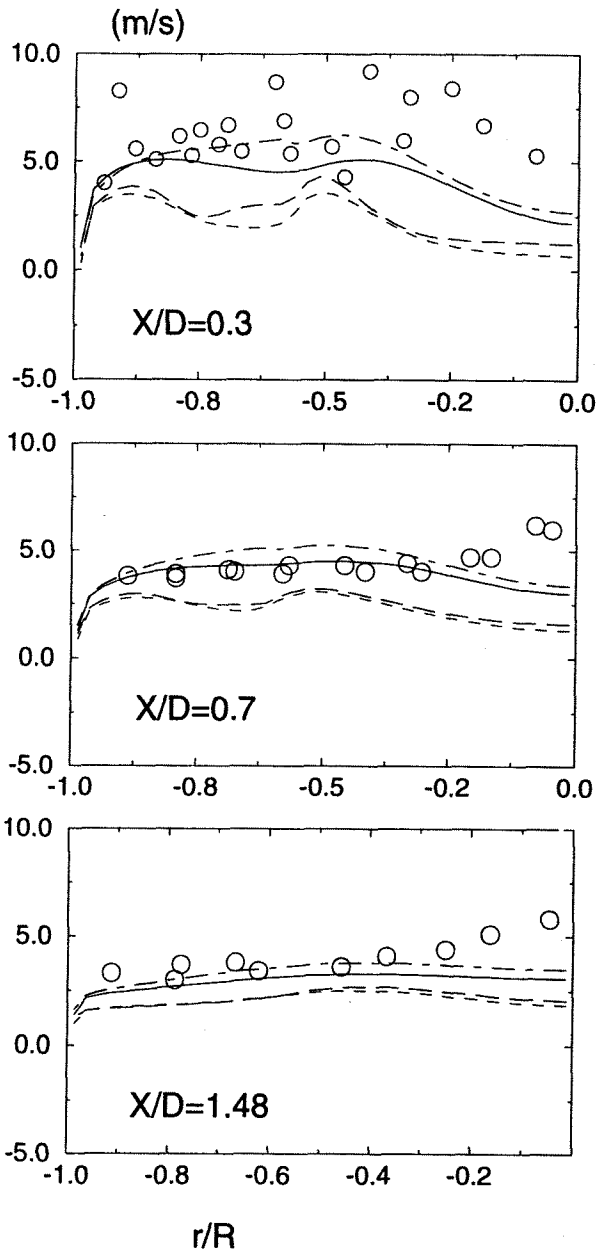

Figure 5: rms axial velocity fluctuations along the radial direction at axial positions $x/D = 0.3, 0.7$ and 1.48. The captions of the different lines and symbols are identical to those in Fig.3.

Fig.5 shows the root-mean-square (rms) of the axial velocity fluctuations, i.e., $\sqrt{\widetilde{u''^2}}$ and Fig.6 shows the rms of the tangential velocity fluctuations ($\sqrt{\widetilde{w''^2}}$). As seen, the computed results are in fairly good agreement with the measurements. The inlet turbulent intensity level has a relatively larger influence on the results than

the two $k-\epsilon$ models do. Under the inlet turbulent intensity $I = 20\%$, the nonlinear $k-\epsilon$ model gives sightly better $\sqrt{\widetilde{u''^2}}$ and $\sqrt{\widetilde{w''^2}}$ as compared with the measurements.

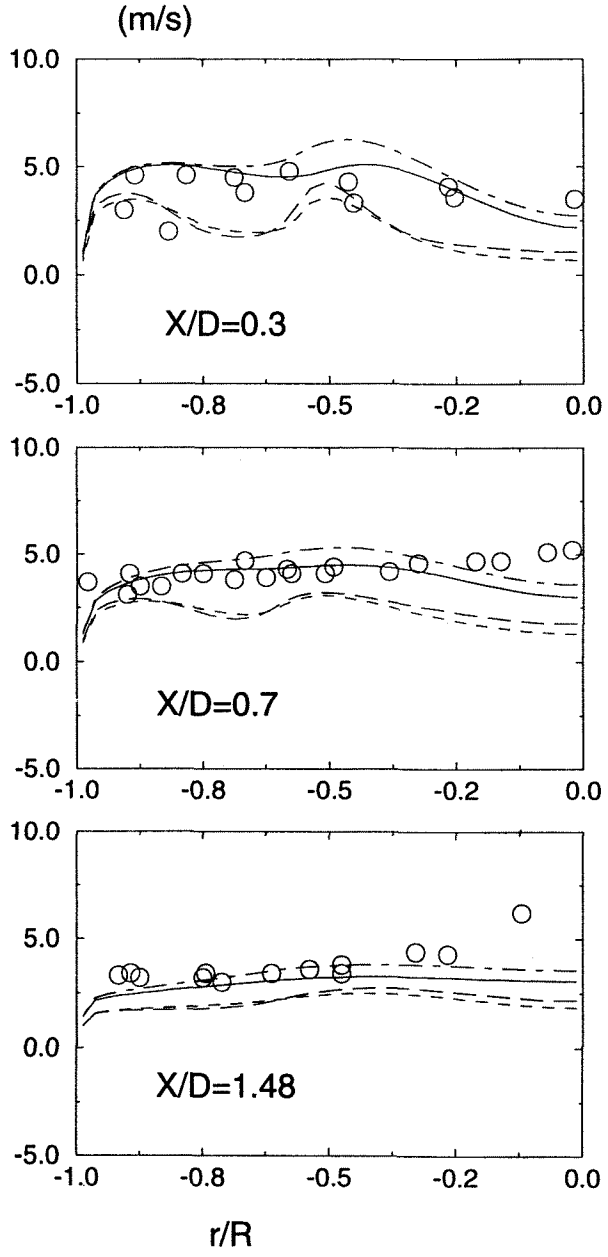

Figure 6: rms tangential velocity fluctuations along the radial direction at axial positions $x/D = 0.3, 0.7$ and 1.48. The captions of the different lines and symbols are identical to those in Fig.3.

3.2 LES RESULTS

In the $k-\epsilon$ calculations a steady state mean axisymmetric flow field was computed. The measurements show that the turbulent field is non-isotropic and swirl affects also the *mean* flow field. These effects cannot be treated be treated within the $k-\epsilon$ framework. In order to compute highly swirling flows, LES is employed. LES calculations yield reasonable results, even though the demands on computer capacities are high. In order to obtain correct LES results, the grid size should be in the order of the Taylor microscale. One may check if the resolution was great enough after the LES calculations. Here, a pre-calculation estimation using energy cascade theory is performed. In this case the Reynolds number based on the integral scales is in the order of 10^5, we must have, in the radial direction, at least 150 grid points in order to have resolution close to the Taylor microscales. The total number of grids in the calculation is about 2 million. Fig.7 shows an instantaneous velocity field (iso-speed contours) at an early time. The result is for isothermal flows in the same combustor under the same swirling condition. As seen, the velocity field is asymmetric. Further evaluation of these LES calculations require more data to compute reliable turbulent statistics. Also, application of LES for reacting flows is currently underway.

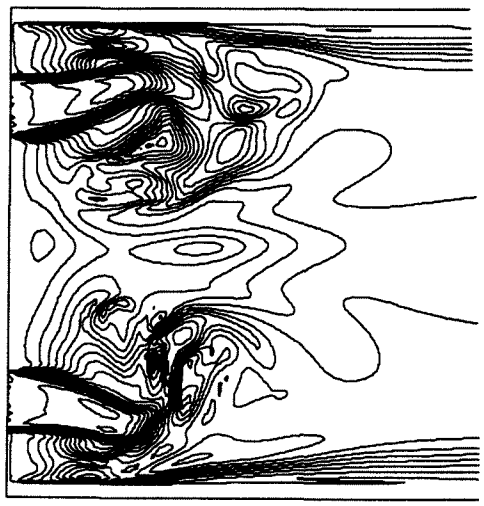

Figure 7: An early-time instantaneous iso-speed contours in the axisymmetric plane of the combustor computed by LES. The flow is isothermal, at pressure 3.9 atm and swirl number 0.3.

4 CONCLUDING REMARKS

In this work, the linear and nonlinear $k-\epsilon$ model are used for the calculation of turbulent reacting flows in a cylindrical combustor with swirling inflows. By comparing with the experimental data, it has been shown that:

1. The mean tangential velocity component is qualitatively well predicted by the $k-\epsilon$ models, while the axial velocity component and the backflow regions are poorly predicted.

2. The rms velocity fluctuations computed by both $k-\epsilon$ models are in qualitative agreement with the experimental data.

3. The results of the linear $k-\epsilon$ and nonlinear $k-\epsilon$ models do not differ much, while the inlet turbulent properties have a fairly large influence on the results.

Preliminary LES calculations on the same combustor are carried out for non-reacting flows. The results show unsteady, asymmetric velocity fluctuations.

ACKNOWLEDGEMENT

This work is supported by NUTEK (the Swedish National Board for Industrial and Technical Development).

REFERENCES

[1] Owen, F.K., Spadaccini, L.J. and Bowman, C.T., "Pollutant Formation and Energy Release in Confined Turbulent Diffusion Flames". 16th Symposium (Int.) on Combustion, 1976, pp. 105-117.

[2] Ribeiro, M.M. and Whitelaw, J.H., "Coaxial jets with and without swirl", Journal of Fluid Mechanics, vol. 96, part 4, 1980, pp. 769-795.

[3] Fu, S., Huang, P.G., Launder, B.E. and Leschziner, M.A., "A comparison of algebraic and differential second-moment closures for axisymmetric turbulent shear flows with and without swirl", Transactions of ASME Journal of Fluid Engineering, vol.110, 1988, pp.216-221.

[4] Lumley, J.L., "Towards a turbulent constitutive relation", Journal of Fluid Mechanics, vol. 41, part 2, 1970, pp. 413-434.

[5] Pope, S.B., "A more general effective-viscosity hypothesis", Journal of Fluid Mechanics, vol. 72, part 2, 1975, pp. 331-340.

[6] Speziale, C.G., "On nonlinear $k-l$ and $k-\epsilon$ models of turbulence", Journal of Fluid Mechanics, vol. 178, 1987, pp. 459-475.

[7] Magnussen, B.F. and Hjertager, B.H., "On Mathematical Modeling of Turbulent Combustion with Special Emphasis on Soot Formation and Combustion", 16th Symposium (Int.) on Combustion, The Combustion Institute, 1976, pp. 719-729.

[8] Pope, S.B., "Computations of Turbulent Combustion: Progress and Challenges", 23rd Symposium (Int.) on Combustion, the Combustion Institute, 1990, pp. 591-612.

[9] Peters, N., "Laminar Diffusion Flamelet Models in Nonpremixed Turbulent Combustion", Progress in Energy and Combustion Science, Vol. 10, 1984, pp. 319-339.

[10] Bai, X.S. and Fuchs, L., "Sensitivity Study of Turbulent Reacting Flows Modeling in Gas Turbine Combustors", AIAA Journal, vol. 33, No.10, 1995, pp. 1857-1864.

[11] Olsson, M. and Fuchs, L., "Large eddy simulation of the proximal region of a spatially developing circular jet". in print, Phys. fluids, 1996.

[12] Germano, M., Piomelli, U., Moin, P. and Cabot, W., "A dynamic subgrid-scale eddy viscosity model", Physics of Fluids A, vol.3, 1991, pp.1790.

[13] Fuchs, L., "An Exact SGS-model for LES". Proc. of the 6th European Turbulence Conference, 1996, to appear.